Article type: Full Paper SMALL

Title: Suspended Silicon Micro-photodiodes for Electrochemical and Biological Applications

Carolina Vargas-Estevez, Marta Duch, Marcos Duque, F. Javier del Campo, Lilian Enriquez-Barreto, Gonzalo Murillo, Núria Torras, José A. Plaza, Carlos A. Saura, Jaume Esteve**

Carolina Vargas-Estevez, Marcos Duque, Marta Duch, Dr. Javier del Campo, Dr. Nuria Torras[┼], Dr. Gonzalo Murillo, Prof. José A. Plaza, Prof. Jaume Esteve
Micro and Nano-Tools group
Instituto de Microelectrónica de Barcelona IMB-CNM (CSIC)
Campus UAB, Bellaterra, 08193, Spain.
E-mail: jaume.esteve@imb-cnm.csic.es

Dr. Lilian Enriquez-Barreto, Prof. Carlos A. Saura
Neurobiology of Alzheimer's disease lab
Institut de Neurociències (INc)
Departament de Bioquímica i Biologia Molecular
Centro de Investigación Biomédica en Red Enfermedades Neurodegenerativas (CIBERNED)
Universitat Autònoma de Barcelona
Bellaterra, 08193, Spain.
E-mail: carlos.saura@uab.cat

[┼] Dr. Nuria Torras present affiliation:
Biomimetic Systems for Cell Engineering Group
Institute for Bioengineering of Catalonia, IBEC
Helix Building, P1, LabA01
c/Baldiri Reixac, 15-21
Barcelona, 08028, Spain

Keywords: suspended microparticles, cell stimulation, photovoltaic cells, neurons, intracellular chips

Local electric stimulation of tissues and cells has gained importance as therapeutic alternative in the treatment of many diseases. These alternatives aim to deliver a less invasively stimuli in liquid media, making imperative the development of versatile micro and nanoscale solutions for wireless actuation. Here, a simple microfabrication process is presented to produce suspended silicon micro-photodiodes that can be activated by visible light to generate local photocurrents in their surrounding medium. Electrical characterization using electrical probes confirms their diode behavior. To demonstrate their electrochemical behavior, an indirect test is performed in solution through photo-electrochemical reactions controlled by a white-LED lamp. Furthermore, their effects on biological systems are observed *in vitro* using mouse

primary neurons in which the suspended micro-photodiodes are activated periodically with white-LED lamp, bringing out observable morphological changes in neuronal processes. The results demonstrate a simplified and cost-effective wireless tool for photovoltaic current generation in liquid media at the microscale.

Introduction

Microelectromechanical systems (MEMS) technologies have enabled the development of multifunctional devices that reach complex functionalities at micro- and nanoscale.[1] Over the recent years, these systems benefited from experience and developments achieved in silicon-based devices to go further in complexity and functionalities.[2] The reduced dimensions of these devices and their fabrication in a clean ambient with biocompatible materials enabled their introduction into the biological field (BioMEMS), with applications like cellular labeling,[3] intracellular sensing[4] or single-cell analysis.[5] In the race to achieve versatile functionalities with reduced dimensions, micro- and nanoparticles have emerged as new tools reaching roles that go from electrochemical detection of biological reactions,[6] to more active roles in wastewater treatment[7] or in the stimulation of living cells.[8,9]

On the other hand, another important feature of functional microtools is the possibility to be activated remotely, especially in liquid media. The problems associated with powering through cables and managing the activation have spurred the search for creative ways of powering and controlling these microsystems.[10] The most interesting solutions have come along with the development of energy harvesters able to generate electricity from external sources, or even turn the available energy in the surrounding media.[11] In terms of photovoltaic energy harvesters, interesting applications have been developed for environmental [12,13] and medical applications.[14,15] The trend in biological photovoltaic applications points toward the development of optical implants, as these active devices convert instantaneously the incident light into electric stimuli, avoiding the complexity of storage and control systems.[16–18] Nevertheless, developments are still evolving in terms of

miniaturization, modularity, independence of action and positioning in order to avoid the issues of surgical interventions thanks to the direct injection of the microdevices in the place of action.[19,20]

Here, we propose the development of novel suspended modular silicon-based micro-photodiodes. Their reduced dimensions (3 µm × 3 µm × 3 µm) and the fabrication process following the standard semiconductor technology with a single photolithographic step, allowed us to create a simple and cost-effective microtool able to act in liquid media. We present the characterization of the microdiodes, and we discuss the potential use of these devices in cellular stimulation, demonstrated through an *in vitro* test with mouse embryonic neurons.

Results and Discussion

Fabrication of microdiodes

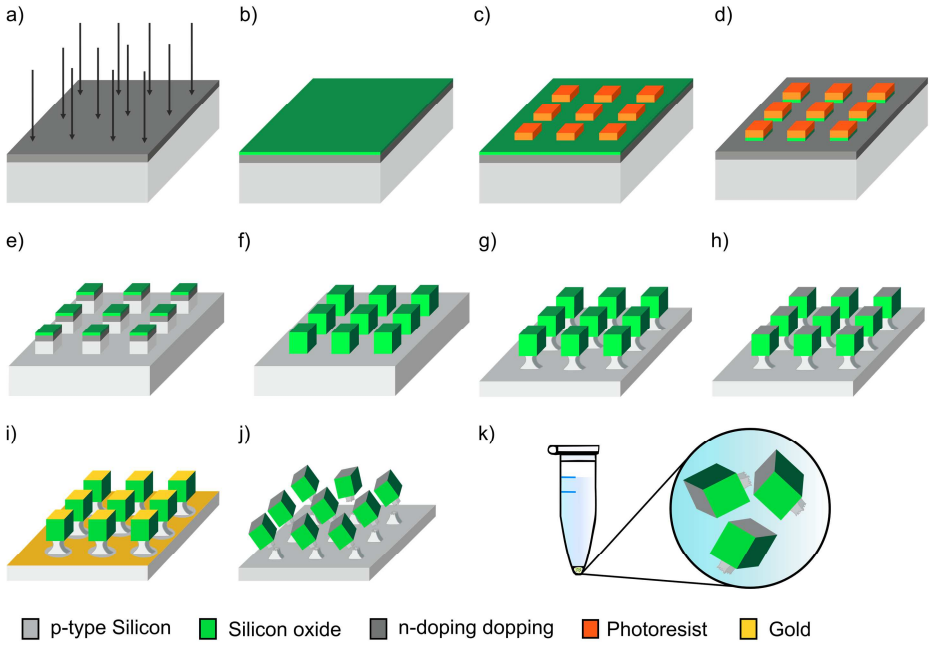

Figure. 1. **Schematic fabrication process of the silicon microdiodes.** a) n-doping implantation of phosphorous on p-type silicon wafer. b) Silicon oxide layer deposited on the top. c-d) Photolithographic patterning followed by e) DRIE to define the microparticle. f) Thin silicon oxide layer deposited to protect the diode and etched from the substrate by highly directional DRIE. g) Isotropic DRIE to create anchors to release the devices. h) A wet etching was performed to remove the top silicon oxide. i) Some samples were evaporated with a top gold layer. j) Mechanical fracture of the anchor to release the microparticles, k) collected and suspended in ethanol.

Figure 1 illustrates the fabrication process of the silicon micro-photodiodes. The process starts with an n-doping ionic implantation of phosphorus onto a four-inch p-type silicon wafer (Figure 1a). The implantation was performed with a dose of 4×10^{15} at/cm^2 and 50 keV of energy. Then, an 800 nm-thick SiO_2 layer was deposited by plasma-enhanced chemical vapor deposition (PECVD) (Figure 1b), followed by an annealing step at 950 ºC for 15 minutes. A photolithographic process was done to define 3 µm x 3 µm structures with a separation of 3 µm between them (Figure 1c). The silicon oxide layer was patterned by reactive ion etching (RIE) (Figure 1d) to act as a mask for a vertical deep reactive ion etching (DRIE) of silicon using the Bosch process[21] to produce 3 µm height pillar structures (Figure 1e). The pillars were covered by a 50 nm PCVD silicon oxide layer to protect the p-n union, which was etched at the substrate by a highly directional anisotropic RIE (Figure 1f). Next, the silicon substrate was partially isotropically etched to obtain a thin anchor with a diameter smaller than 1 µm (Figure 1g). Finally, the top layer of silicon oxide on the particles was removed by a short hydrofluoric acid solution wet etching (Figure 1h). Optionally, a 50 nm thick gold layer was evaporated on some of the samples to improve the electrical output of the micro-photodiode for the electrical characterization in substrate (Figure 1i). Finally, microparticles were released from the substrate by the mechanical peel-off process described in detail in ref. [5] (Figure 1j), collected and re-suspended in ethanol for their storage (Figure 1k). The microparticles were 4 µm height after being release as part of the anchor stay with the particle. The density of the devices in suspension was around 1.5 x 10^6 micro-photodiodes per milliliter of ethanol.

The morphology of the micro-photodiodes was observed by scanning electron microscopy (SEM). **Figure 2a** shows a micro-photodiode with its thin anchor fractured. The width of the anchor was established around 1 µm, confirmed with a transversal cut performed by Focused Ion Beam (FIB) (Figure 2b). This cross-section also shows the good adhesion of the SiO_2 passivation layer and how it covers the junction properly. The optional samples fabricated for

electrical test had isolated electrodes due to the anisotropically nature of the evaporation technique used for the metallization, without the need of an additional mask (Figure 2c). The layer on the top of the particle established the n-junction contact while the remaining layer on the substrate enables to contact the p-junction contact. In order to determine the depth junction, numerical simulations were done with the software TCAD Silvaco Atlas. Thanks to this advanced virtual wafer-fabrication tool, using the fabrication conditions, including the dopants, the energy used to create the n-region in the p-silicon wafer and the annealing parameters, the junction was established to be around 0.56 µm (Figure 2d). Additionally, the junction was also delimited through wet-chemical etching of the silicon. This hydrofluoric/nitric/acetic acid system, based on the different etching rates in p-doped and n-doped areas, delimitated the junction in 560 ± 10 nm which agrees with the previous simulation (Figure 2e).

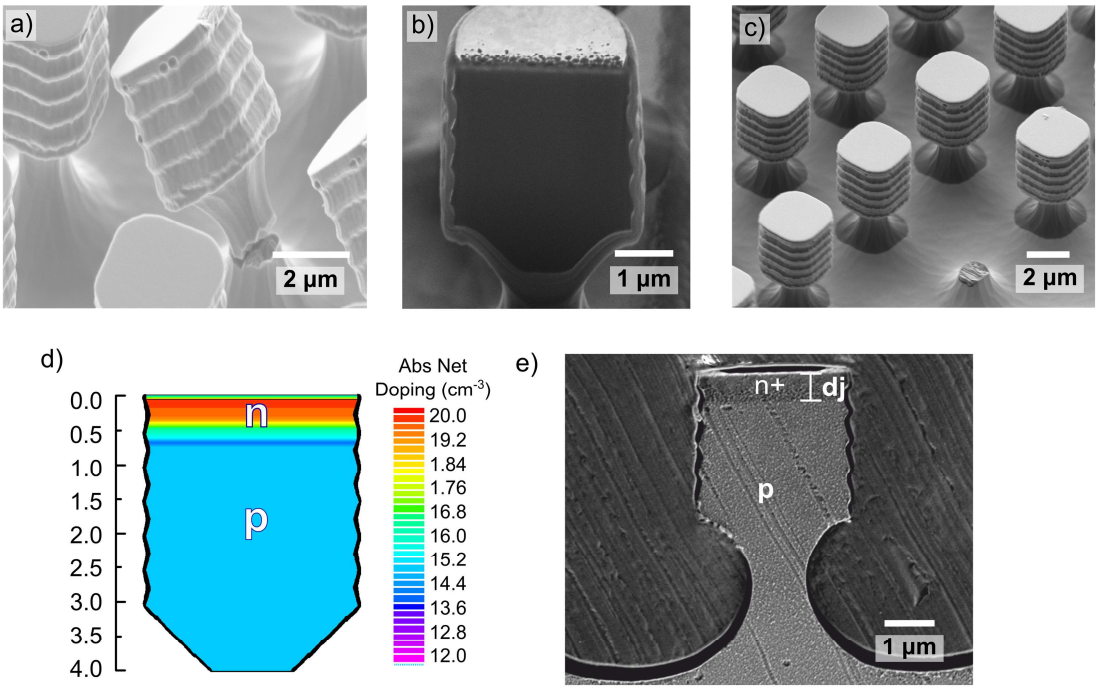

Figure. 2. SEM images of a) bare silicon micro-photodiodes fabricated, b) cross section milled by FIB and c) micro-photodiodes with the thin top layer of gold. d) Doping profile simulated in TCAD Silvaco Atlas. e) SEM image of the wet-etched junction. *dj*: depth of the junction 560 ± 10 nm

Photo-electrical characterization of the micro-photodiodes

Experimentally, the output characteristic was measured through a FIB—SEM featuring an electric probe. A single micro-photodiode, still attached to the substrate, was isolated by milling the surrounding structures by FIB (**Figure 3a**). The anode on the substrate was contacted by a clamp and the cathode, at the top, was contacted carefully with the probe tip (Figure 3b). The bias voltage used was ranged from -3 V to 3 V. The I-V curve obtained is shown in Figure 3c, which confirmed the correct behavior of the diode.

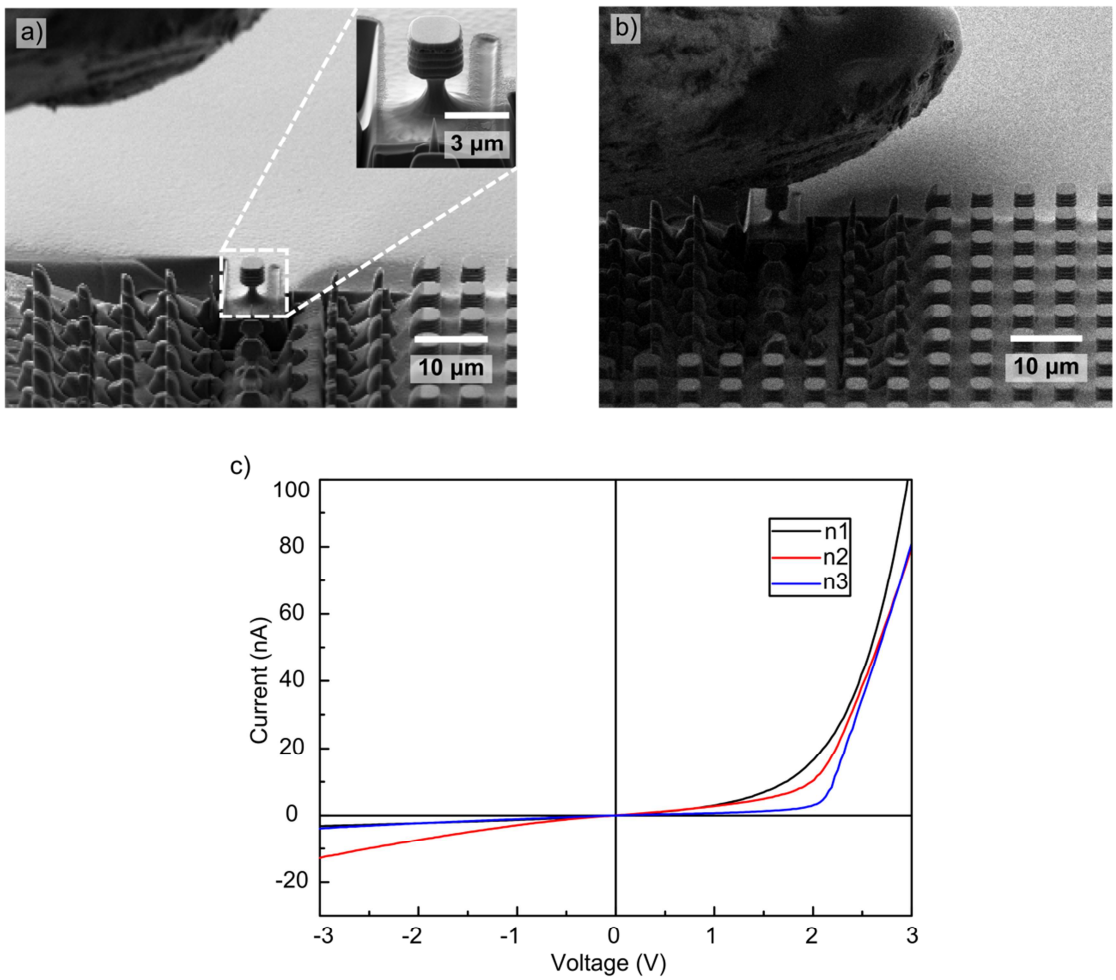

Figure. 3. SEM image of a) the micro-photodiode isolated by FIB milling and b) contacted by an electrical probe. c) Experimental output obtained using a bias voltage of +/-3V in three different isolated micro-photodiodes.

The microdiode presented a forward voltage of around 0.3 V, and a relatively linear reverse V-I curve with a large breakdown voltage. This gradual knee corresponds to the expected behavior for a thin junction device. No saturation region was obtained experimentally due to the parasitic resistances associated to the device arising from the fabrication process.

The temporal response of the device at 0 V bias voltage, under light and dark conditions, was studied using an AFM electrical probe. Illumination was performed by 150 W quartz-halogen fiber optic illuminator, attached to the AFM microscope, additional to the light coming from the laser of the AFM microscope. The electrical response was defined by the tip in contact with the top of the microdevice, anode, (**Figure 4a**) and the cathode, defined by a clamp attached to the substrate. The photovoltaic effect exhibited by the diode is shown in Figure 4b, in black with the light off and in red with the light on, confirming the generation of a photocurrent due to the photoelectric effect in the junction.

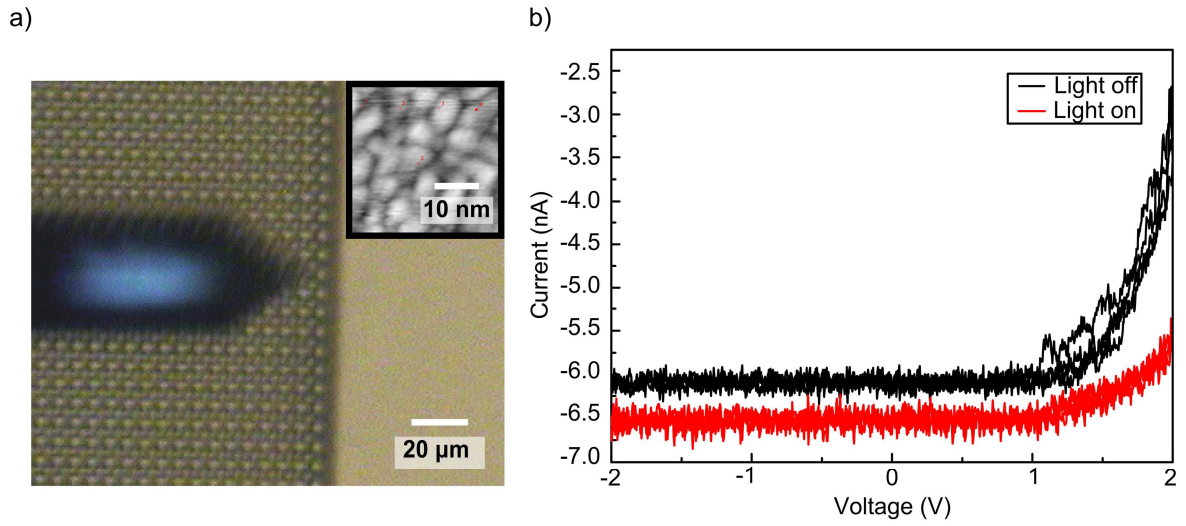

Figure. 4. Optical image of the a) AFM electrical probe contacting one micro-photodiode. The inset corresponds to the AFM image done to set the contact points of the electrical probe. b) Photoresponse of the micro-photodiode obtained by AFM electric probe, under lighting and dark conditions.

Electrochemical activity of the micro-photodiodes

In order to study the performance of micro-photodiodes in solution, an experiment was carried out in solution using ferrocyanide. Ferrocyanide is a stable and colorless iron complex exhibiting reversible oxidation to ferricyanide. In contrast to ferrocyanide, ferricyanide displays an absorption maximum around 420 nm, and can be quantified (ε=1020 M^{-1} cm^{-1}) by spectrophotometry. 1 mM ferrocyanide was put in contact with the photodiodes on their silicon substrate. Afterwards, a white-LED lamp was used to illuminate the photodiodes. The oxidation of ferrocyanide resulted in a color change measurable by UV-Vis spectroscopy.

Because ferrocyanide can be oxidized by ambient oxygen, the experiment was performed in darkness inside a faraday cage under a nitrogen flow. Light was provided by a 150 W halogen cold lamp along with dual gooseneck light guides placed facing the top part of the diodes (**Figure 5a**). The samples used were the bare silicon micro-photodiodes attached to the substrate and an extra sample with a top gold-layer. The solution color change was compared with a control sample of ferrocyanide exposed to the same light conditions but in the absence of the micro-photodiodes.

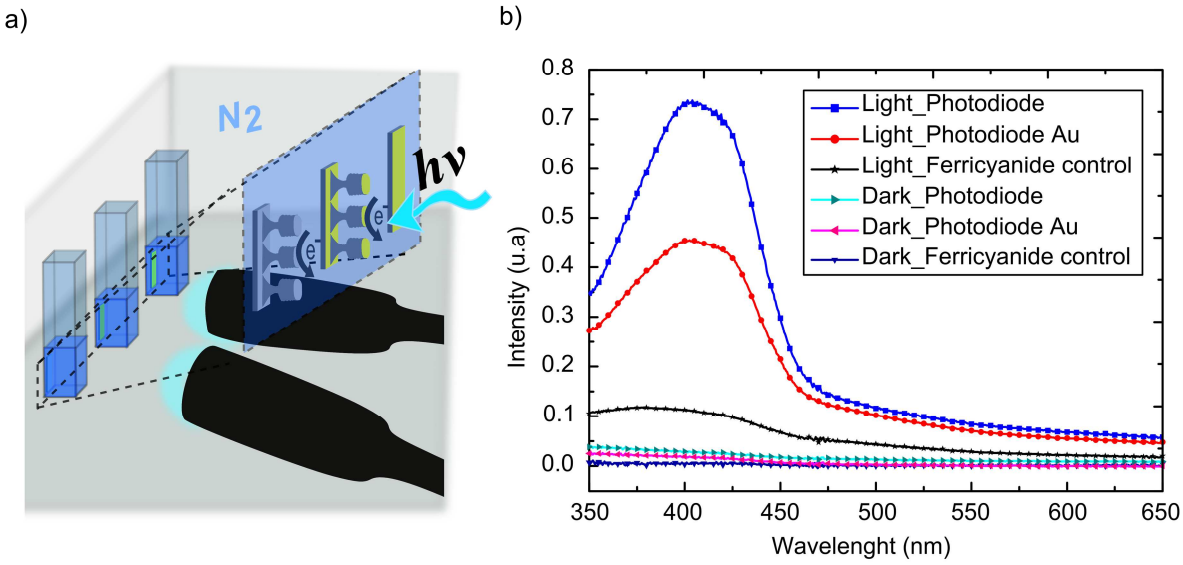

Figure. 5. a) Diagram of the set-up for the electrochemical test with ferrocyanide solution, having a control sample, a chip with the micro-photodiodes and a chip with the micro-photodiodes with the gold layer. b) Electrochemical response of the micro-photodiodes in a REDOX ferrocyanide system activated by an intense with light.

The results demonstrate the effect of the microdiodes in solution once they are activated. As Figure 5b shows, light absorption at 420 nm (due to ferricyanide) is higher in the presence of the photodiodes than in the control sample. Surprisingly, the diodes with a gold electrode LED to the production of less ferricyanide than those without one electrode coated with gold. One possible explanation could be that the gold electrode improves the electron transfer properties, and part of the ferricyanide produced at the anode (p-doped side) is converted back to ferrocyanide at the gold electrode (in contact with the n-doped side). In the absence of a

gold layer, the photocurrent transfer from the n-doped silicon to the solution is significantly slower, allowing the ferricyanide produced at the anode to escape by diffusion into the solution bulk, and leading to the observation of more color. Another possibility is that the smooth gold surface reflects the light vertically, reducing drastically the generation of carriers in the junction. Given that the photodiodes without gold were apparently more active, subsequent experiments were carried out without gold.

Biological applicability of the micro-photodiodes

As an initial proof-of-concept of the use of the stimulation produced by these suspended photovoltaic microdiodes for bioapplications, we performed *in vitro* cell biology assays in cultured neurons.

It is well established that neuron growth, proliferation, differentiation and migration is dependent on neuron-neuron communication, and that electrical activity has a key role in these complex processes.[22] Neurons in culture develop cell processes, including axons and dendrites, which are positive for MAP2 protein, and synaptic contacts.[23] Neuron branching is dependent on the ionic stimulus of the surrounding environment, especially with neighboring communication between neurons, through calcium signaling that can affect the number and/or length of neuronal processes.[23] Primary cortical neurons obtained from mouse embryonic brains were cultured for 2 days in growing medium before adding the micro-photodiodes. The effects of photovoltaic microdiodes were analyzed after 2 days of incubation with them in lighting or dark conditions applied by a white-LED portable lamp compared to control neurons under the same conditions (**Figures 6a**). In these conditions, SEM imaging revealed that microdiodes efficiently bound to the cell surface of cortical neurons, especially at soma but also along processes (Figures 6b-c). We next, examined morphological changes of dendrites of neurons grown in the absence (control) or presence of micro-photodiodes in conditions of illumination by performing immunofluorescence staining of MAP2 and

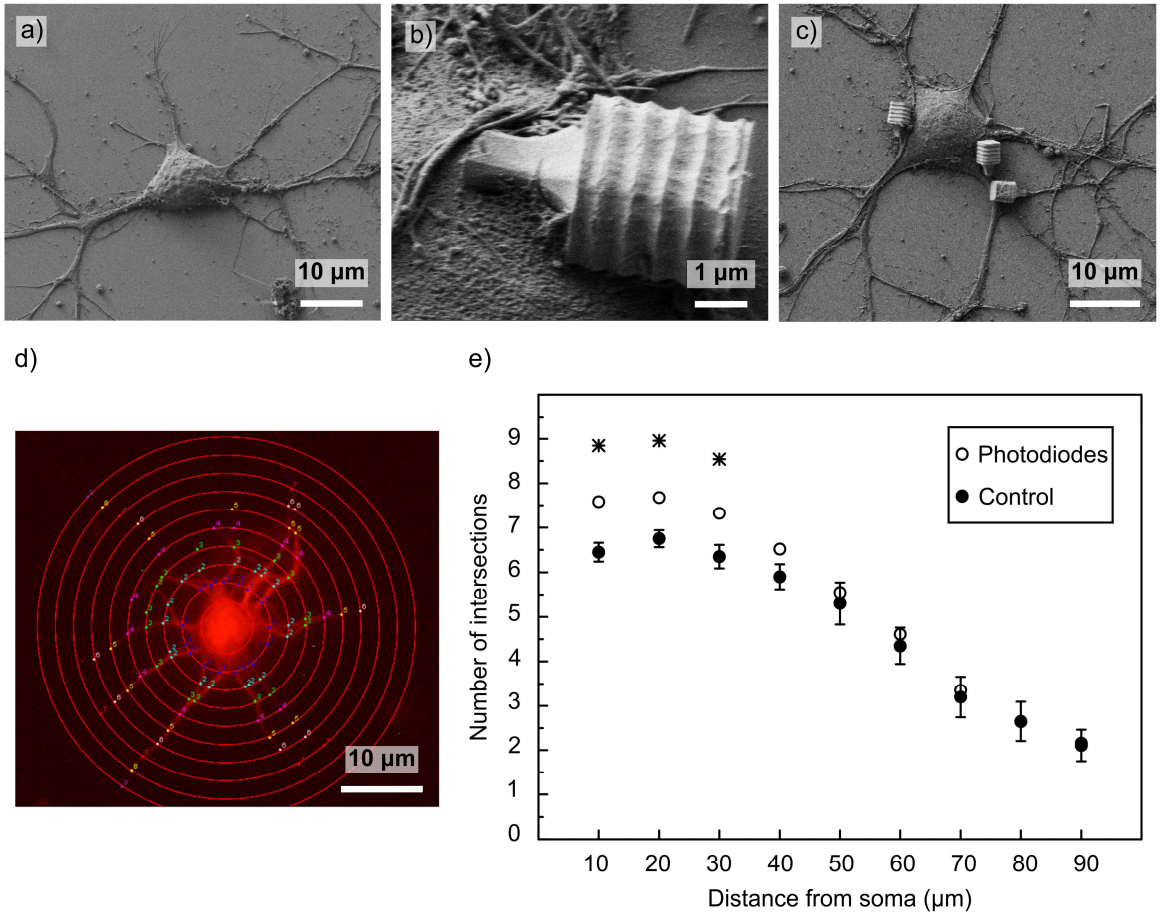

Figure. 6. SEM images under white-LED lamp illumination of a) control neuron (left), b) neuron with a photodiode attached to soma (middle) and c) neuron with photodiodes attached to dendrites (right). d) Example of Sholl analysis of cultured neurons stained with MAP2 antibody (red) and incubated in the presence of photodiodes after illumination. e) Intersections of dendrites with concentrical circles at increasing radius under illumination were quantified. (*Denotes statistical difference $P < 0.05$ vs control)

fluorescence imaging. Dendritic morphology was studied using Sholl analysis[24] by comparing the number of branch intersections every 10 µm from the cell soma (Figure 6d). Analysis of circle intersections revealed a significant increase in the number of short-distance dendrites (radius ranged from 10-30 µm) but unchanged number of long-distance dendrites (radius ranged from 40-90 µm) in neurons with micro-photodiodes (Figure 6e). This result suggests that microdiodes favor dendritic complexity by increasing the number of proximal dendrites of cultured neurons.

Conclusion

In summary, silicon micro-photodiodes were fabricated by ionic implantation of phosphorus atoms over a silicon substrate, and a sequence of DRIE processes with a single

photolithographic mask. These structures were fabricated with a thin anchor that allowed a clean, effective and simple way to release them and collected them in suspension. Electrical characterization showed the characteristic diode curve as expected. Furthermore the photovoltaic behavior in liquid was validated through a redox system with ferrocyanide, showing a visible effect created by the photocurrent interacting with the surrounding media. As a proof of concept of this photocurrent effect, an *in vitro* study in cultured neurons under lighting or dark conditions was held. Interestingly, morphological changes in neuronal processes of cultured neurons were observed with the micro-photodiodes under lighting conditions. Further work is ongoing to improve the design, efficiency and fabrication process. Likewise, there is still a path ahead to explore these proposed micro-photodiodes as remote photovoltaic cells for life science applications in the years to come.

5. Experimental Section

Electrical measurements: Electrical measurements were carried out in two different ways. The first test was carried out in a combined dual beam, Focused Ion Beam (FIB)—Scanning Electron Microscopy (SEM, Leo 1530 Zeiss, Germany) with a Gemini SEM column, provided with an electric probe. Next a single photodiode, still attached in the silicon platform, was isolated using the ion beam of the FIB to mill the diodes around it. A layer of thermally evaporated 5 nm thick Cr / 50 nm thick Au, deposited before the milling, was used as electrodes. The process took advantage of the shadow created by the pillar to establish a cathode electrode over the platform and anode electrode at the top of the micro-photodiode. The probe was slowly approached and using the direct voltage mode, the contact between the probe and the micro-photodiode was confirmed. Next, with a bias voltage ranging from -3 V to 3 V, the I-V curve was acquired. The second test was carried out using the electrical probe of an atomic force microscope (AFM, Agilent 5500 AFM system, USA). A sample of the fabricated micro-photodiodes on the substrate and the gold electrode deposited was contacted

by the probe on the top of one microdiode. A bias voltage ranging from -2 to 2 V was applied to polarize the diode and observe the I-V characteristic curve. Furthermore, an additional light source of 150 W quartz halogen fiber optic illuminator (Fiber-Lite MI-150, Dolan-Jenner, USA), was used to observe the dark current mode. As the whole system was enclosed in a dark cage, the dark condition was established switching off the additional light source.

Electrochemical setup: UV-Vis spectroscopy analysis was performed using ferrocyanide redox reaction along with the micro-photodiodes in substrate in DU®730 Life Science UV/Vis Spectrophotometer (Beckman Coulter Inc., Fullerton, Calif., U.S.A.). The absorbance was measured from 350 nm to 650 nm. A solution of 2 mM $[Fe(CN)_6]^{4-}$ in 0.1 mM KNO_3 was prepared fresh before each experiment. The solution with each type of substrate was placed in a quartz cuvette inside a dark chamber along with another quartz cuvette with only ferrocyanide solution as control. The illumination was performed with 150 W halogen lamp using dual goose-neck light guides powered by CL 1500 ECO cold light source (Zeiss, Germany). The light guides had an active diameter of 4.5 mm. The chamber was filled with nitrogen to reduce the oxidation speed due to the environment.

Neural cell culture: Brains from fifteen day-old wild-type (WT) mouse embryos were used to obtain primary cortical neurons. The brains were transferred to PBS, meninges were removed and cortical tissue was dissected. Cortical tissues were then placed in Krebs–Ringer bicarbonate (KRB) buffer, with bovine serum albumin (0.5 % w/v, BSA, Sigma, A7906) and centrifuged at 1500 rpm. Then, the solution was supplemented with trypsin (Gibco, USA), incubated for 10 minutes at 37 °C, and followed by trypsin inhibitor (Sigma, USA) to stop reaction, along with a DNAse solution. Afterwards, the tissue is mechanically dissociated with a Pasteur pipette, filtered and suspended in Dulbecco's Modified Eagle Media (DMEM, Thermo Fisher Scientific, USA) supplemented with 50 ml fetal bovine serum (HyClone, USA), 10 ml glucose (Sigma, USA), 5 ml L-glutamine (Gibco, USA), and 2.5 ml Penicillin/Streptomycin (Gibco, USA). The neuronal cell suspension was plated at a density of

150 000 cells/cm^2 on coverslips precoated with poly-d-lysine (0.1 mg/ml; Sigma, USA) in 24-well plates. The cell culture was maintained at 37 °C in 5% CO_2. The medium was replaced every 4 DIV with neurobasal medium (Gibco) supplemented with B27 (50X, Invitrogen), 5 ml L-glutamine, and 2.5 ml Penicillin/Streptomycin. Experimental procedures were conducted according to the Animal and Human Ethical Committee of the Universitat Autònoma de Barcelona (CEEAH 1783 and 2896) following the European Union guidelines (2010/63/EU)

Cell stimulation: Cell culture media solutions containing the micro-photodiodes in concentrations of 300 k, 200 k and 100 k were added into cultured cortical neurons (2 DIV) and activated with light from the third day to the fifth day of incubation. The light source was established with a 1.25 W white-LED lamp (95-111 Mini Tripod Flashlight, Stanley, USA) with a maximum intensity light spot around 1.6 cm. The cell plates were taken out of the incubator and illuminated with the white-LED lamp in lapses of 1 minute every 10 minutes for one hour, so that way we completed 6 photo-stimulations per day. Cells were fixed at 6 DIV for further analysis.

SEM characterization of cells after stimulation: Samples for SEM were rinsed three times in phosphate buffered (PB: 0.1 M, pH 7.4), fixed in 2.5% glutaraldehyde (EM grade, Merck, Darmstadt, Germany) in PBS for 15 minutes at room temperature (RT) and rinsed four times in PBS. Then the cell culture was post-fixed for 2 h with osmium tetroxide (TAAB Lab., UK), with 0.7 % ferrocyanide in PBS, followed by a rinse with DI water. Cell dehydration was performed in ascending series of ethanol (50% once, 70% twice and 90% three times, and three times in 100%), 10 min each. Finally, samples were critical point dried via CO_2 of highest purity (K850 critical point drier Emitech), mounted on stubs and analyzed using SEM (Merlin, Carl Zeiss, Germany).

Immunofluorescent labeling of cells after stimulation: Cortical neurons were washed with PBS three times, fixed with paraformaldehyde (4% w/v, EM grade, Merck, Darmstadt, Germany) for 10 minutes at RT, permeabilized and blocked with a blocking buffer (0.2% Triton-x/PBS,

2% bovine serum albumin, 2% goat serum, 0.05% azide) for 30 min. Cells were incubated with the monoclonal anti-MAP2 antibody (1:300, Sigma-Aldrich, M4403) followed by secondary goat Alexa Fluor 568 anti-mouse IgG (1:300, Molecular Probes Inc., Eugene, OR, USA) and the nuclear marker Hoechst (1:5000, Thermo Fisher Scientific, MA, USA). Finally, following PBS rinses, cells were placed over mounting media Mowiol (Sigma, USA) on a rectangular glass slide to being analyzed with the fluorescence microscope (Nikon Eclipse 90i, Nikon, Tokyo, Japan).

Sholl analysis: Neuronal branching complexity was analyzed at 6 DIV. 40X magnification pictures from isolated neurons were digitally enhanced and analyzed using the "Concentric Circles" plugin from ImageJ software. Thus, a series of concentric circles were drawn, centered on the cell body and gradually increasing in diameter in 10 µm steps. A two-dimensional analysis was performed, counting the number of branches that intersected the successive circles.[24] A t-test Student analysis was performed to compare the number of crossings every 10 µm in neurons in control samples and in samples with micro-photodiodes. Data represent average (± SEM) of multiple neurons in duplicate/triplicate coverslips in control (n=20) and photodiodes (n=32) conditions. $P < 0.05$ was considered statistically significant.

Supporting Information

Supporting Information is available from the Wiley Online Library or from the author.

Acknowledgements

We thank members of the Clean Room staff of IMB-CNM for the help in the fabrication of the micro-photodiodes. In addition, we would like to thank Dr. Neus Domingo from the Catalan Institute of Nanoscience and Nanotechnology, ICN2, for performing the AFM measurements. This research was supported by a Spanish government through the project MINAHE 5 (TEC2014-51940-C2), EU ERDF (FEDER), the predoctoral FPI grant (BES-2012-052105) to CVE and the TRANSMECAD grant to CAS (SAF2013-43900-R) from the Ministerio de Economía, Industria y Competitividad of Spain.

References

[1] C.M. Ho, Y.C. Tai, *Annu. Rev. Fluid Mech* **1998**, *30*, 579.

[2] M. Tilli, A. Haapalinna, in *Handb. Silicon Based MEMS Mater. Technol.*, Elsevier,

2015.
[3] S. Durán, M. Novo, M. Duch, R. Gómez-Martínez, M. Fernández-Regúlez, A. San Paulo, C. Nogués, J. Esteve, E. Ibañez, J. A. Plaza, *Lab Chip* **2012**, 6, 1508.
[4] R. Gómez-Martínez, A. M. Hernández-Pinto, M. Duch, P. Vázquez, K. Zinoviev, E. J. de la Rosa, J. Esteve, T. Suárez, J. A. Plaza, *Nat. Nanotechnol.* **2013**, 8, 517.
[5] N. Torras, J. P. Agusil, P. Vázquez, M. Duch, A. M. Hernández-Pinto, J. Samitier, E. J. De La Rosa, J. Esteve, T. Suárez, L. Pérez-García, J. A. Plaza, *Adv. Mater.* **2016**, *28*, 1449.
[6] R. Popovtzer, T. Neufeld, E. z. Ron, J. Rishpon, Y. Shacham-Diamand, *Sensors Actuators B Chem.* **2006**, *119*, 664.
[7] S. K. Srivastava, M. Guix, O. G. Schmidt, *Nano Lett.* **2016**, *16*, 817.
[8] X. Sui, J. Sun, L. Li, C. Zhou, X. Luo, N. Xia, Y. Yan, Y. Chen, Q. Ren, X. Chai, *IEEE Trans. Neural Syst. Rehabil. Eng.* **2013**, *21*, 524.
[9] G. Murillo, A. Blanquer, C. Vargas-Estevez, L. Barrios, E. Ibáñez, C. Nogués, J. Esteve, *Adv. Mater.* **2017**, 1, *1605048*.
[10] A. Yakovlev, S. Kim, A. Poon, *IEEE Commun. Mag.* **2012**, *50*, 152.
[11] K. V. Selvan, M. S. Mohamed Ali, *Renew. Sustain. Energy Rev.* **2016**, *54*, 1035.
[12] S. Y. Reece, J. A. Hamel, K. Sung, T. D. Jarvi, A. J. Esswein, J. J. H. Pijpers, D. G. Nocera, *Science (80-.).* **2011**, *334*, 645.
[13] T. Hisatomi, J. Kubota, K. Domen, *Chem. Soc. Rev.* **2014**, *43*, 7520.
[14] S. Bermejo, S. Silvestre, P. Ortega, *Microelectron. Eng.* **2014**, 119, 109.
[15] D. Boinagrov, X. Lei, G. Goetz, T. I. Kamins, K. Mathieson, L. Galambos, J. S. Harris, D. Palanker, *IEEE Trans. Biomed. Circuits Syst.* **2016**, *10*, 85.
[16] K. Mathieson, J. Loudin, G. Goetz, P. Huie, L. Wang, T. I. Kamins, L. Galambos, R. Smith, J. S. Harris, A. Sher, D. Palanker, *Nat. Photonics* **2012**, 6, 391.
[17] L. Yue, J. D. Weiland, B. Roska, M. S. Humayun, *Prog. Retin. Eye Res.* **2016**, *53*, 21.
[18] E. Zrenner, *Nat. Photonics* **2012**, *6*, 344.
[19] A. Abdo, M. Sahin, D. S. Freedman, E. Cevik, P. S. Spuhler, M. S. Unlu, *J. Neural Eng.* **2011**, *8*, 56012.
[20] J. Liu, T.-M. Fu, Z. Cheng, G. Hong, T. Zhou, L. Jin, M. Duvvuri, Z. Jiang, P. Kruskal, C. Xie, Z. Suo, Y. Fang, C. M. Lieber, *Nat. Nanotechnol.* **2015**, 7, 629.
[21] F. Laermer, A. Schilp, *Method of Anisotropically Etching Silicon*, **1996**.
[22] N. C. Spitzer, *Nature* **2006**, *444*, 707.
[23] F. Tang, K. Kalil, *J. Neurosci.* **2005**, *28*, *6702*.
[24] D. A. Sholl, *J. Anat.* **1953**, *87*, 387.